

The role of orbital dynamics in spin relaxation and weak antilocalization in quantum dots

Oleg Zaitsev,^{1,*} Diego Frustaglia,² and Klaus Richter¹

¹*Institut für Theoretische Physik, Universität Regensburg, D-93040 Regensburg, Germany*

²*NEST-INFM & Scuola Normale Superiore, 56126 Pisa, Italy*

We develop a semiclassical theory for spin-dependent quantum transport to describe weak (anti)localization in quantum dots with spin-orbit coupling. This allows us to distinguish different types of spin relaxation in systems with chaotic, regular, and diffusive orbital classical dynamics. We find, in particular, that for typical Rashba spin-orbit coupling strengths, integrable ballistic systems can exhibit weak localization, while corresponding chaotic systems show weak antilocalization. We further calculate the magnetoconductance and analyze how the weak antilocalization is suppressed with decreasing quantum dot size and increasing additional in-plane magnetic field.

PACS numbers: 03.65.Sq, 71.70.Ej, 73.23.-b

Weak localization (WL) and antilocalization (AL) are classic examples for quantum interference and spin-orbit (SO) interaction effects on the conductance in low-dimensional electronic systems [1, 2]. Very recently, particularly weak AL has been reconsidered in a number of experiments since AL can be employed as a probe of SO-induced spin dynamics and relaxation phenomena. Measurements have been performed both for GaAs- and InAs-based two-dimensional (2D) electron gases [3], as well as for ballistic bismuth [4] and GaAs [5] cavities. While SO scattering in extended disordered systems is well understood [2], the latter experiments address the timely question of how quantum confinement of the orbital motion affects spin relaxation in clean ballistic quantum dots where the elastic mean-free path is much larger than the system size. Considerable related progress has also been made theoretically in treating spin relaxation and the interplay between SO and Zeeman coupling in quantum dots [6] including random-matrix theory (RMT) [7, 8]. However, the RMT results apply only to chaotic quantum dots and contain geometric parameters which must be obtained by other means for a given system.

Here we present an alternative, semiclassical theory for the spin-dependent magnetoconductance of quantum dots, i.e. a semiclassical Landauer formula including spin, and apply it to describe weak AL in 2D confined systems. This approach allows to uncover the interrelation between orbital dynamics and spin evolution in a transparent way, and it is rather generally applicable to quantum dots with different type of classical dynamics, e.g., chaotic and regular. Remarkably, we find significant qualitative differences in the spin relaxation times of chaotic, integrable, and open diffusive systems: Spin relaxation for confined chaotic systems is much slower than for diffusive motion; moreover, for a number of integrable geometries we even find a saturation, i.e., a certain spin polarization is preserved. Furthermore, we examine the effect of the system size and of an additional in-plane magnetic field on the resulting AL.

Our study is based on the semiclassical Landauer for-

mula [9, 10] that we generalize to systems with SO and Zeeman interaction. To this end, we extend techniques for spin semiclassics, recently developed for the density of states [11, 12], to quantum transport. We consider a Hamiltonian linear in the spin operator \hat{s} ,

$$\hat{H} = \hat{H}_0(\hat{\mathbf{q}}, \hat{\mathbf{p}}) + \hbar \hat{s} \cdot \hat{\mathbf{C}}(\hat{\mathbf{q}}, \hat{\mathbf{p}}), \quad (1)$$

where $\hat{\mathbf{C}}(\hat{\mathbf{q}}, \hat{\mathbf{p}})$ is a vector function of the position and momentum operators $\hat{\mathbf{q}}, \hat{\mathbf{p}}$, which may include an external (inhomogeneous) magnetic field. For a large number of systems of interest, and usually in experiments, $\hbar s |\mathbf{C}(\mathbf{q}, \mathbf{p})| \ll H_0$, even if the spin-precession length is of the order of the system size. Here s is the particle spin, and the phase-space functions without a hat denote the classical counterparts (Wigner-Weyl symbols) of the respective operators. As a consequence of the above inequality the influence of spin on the orbital motion can be neglected. Thus H_0 determines the classical trajectories $\gamma = (\mathbf{q}(t), \mathbf{p}(t))$ which, in turn, generate an effective time-dependent magnetic field $\mathbf{C}_\gamma(t) = \mathbf{C}(\mathbf{q}(t), \mathbf{p}(t))$ acting on spin via the Hamiltonian $\hat{H}_\gamma(t) = \hbar \hat{s} \cdot \mathbf{C}_\gamma(t)$. Hence the spin dynamics can be treated *quantum-mechanically* in terms of a (time-ordered) propagator $\hat{K}_\gamma(t) = T \exp[-i \int_0^t dt' \hat{s} \cdot \mathbf{C}_\gamma(t')]$.

To derive a semiclassical expression for the spin-dependent conductance of a quantum dot, we start from the Landauer formula in two dimensions relating the two-terminal conductance $G = (e^2/h)\mathcal{T}$ to its transmission coefficient [13]

$$\mathcal{T} = \sum_{n=1}^{N'} \sum_{m=1}^N \sum_{\sigma, \sigma'=-s}^s |t_{n\sigma', m\sigma}|^2. \quad (2)$$

The leads support N and N' open orbital channels m and n , respectively, and we distinguish $2s + 1$ spin polarizations in the leads, labeled by $\sigma = -s, \dots, s$. In (2), $t_{n\sigma', m\sigma}$ is the transition amplitude between the incoming channel $|m, \sigma\rangle$ and outgoing channel $|n, \sigma'\rangle$; a corresponding equation holds for the reflection coefficient \mathcal{R} satisfying the normalization condition $\mathcal{T} + \mathcal{R} = (2s+1)N$.

A semiclassical evaluation of the transition amplitudes, starting from a path-integral representation of the Green function, yields [14] (see [9] for the spinless case)

$$t_{n\sigma',m\sigma} = \sum_{\gamma(\bar{n},\bar{m})} (\hat{K}_\gamma)_{\sigma'\sigma} \mathcal{A}_\gamma \exp\left(\frac{i}{\hbar} \mathcal{S}_\gamma\right), \quad (3)$$

given as coherent summation over classical paths at fixed energy [15]; corresponding results hold for the reflection amplitudes in terms of back-reflected paths. The sum runs over classical trajectories $\gamma(\bar{n} = \pm n, \bar{m} = \pm m)$ that enter (exit) the cavity at “quantized” angles $\Theta_{\bar{m}}$ ($\Theta_{\bar{n}}$). For hard-wall boundary conditions, $\sin \Theta_{\bar{m}} = \bar{m}\pi/kw$ and $\sin \Theta_{\bar{n}} = \bar{n}\pi/kw'$, where k is the wavenumber, and w, w' are the lead widths. In (3), \mathcal{S}_γ ($= \hbar k L_\gamma$ for billiards) is the action along γ with time T_γ and classical weight \mathcal{A}_γ [9]. The entire spin effect is contained in the matrix elements $(\hat{K}_\gamma)_{\sigma'\sigma}$ of the spin propagator $\hat{K}_\gamma \equiv \hat{K}_\gamma(T_\gamma)$ between the initial and final spin states.

Inserting (3) into (2) we derive the semiclassical Landauer formula for spin-dependent magnetotransport (including SO and Zeeman interaction):

$$\mathcal{T} = \sum_{nm} \sum_{\gamma(\bar{n},\bar{m})} \sum_{\gamma'(\bar{n},\bar{m})} \mathcal{M}_{\gamma,\gamma'} \mathcal{A}_\gamma \mathcal{A}_{\gamma'}^* e^{(i/\hbar)(\mathcal{S}_\gamma - \mathcal{S}_{\gamma'})}. \quad (4)$$

The orbital contribution of each pair of paths is weighted by the spin *modulation factor*

$$\mathcal{M}_{\gamma,\gamma'} = \text{Tr}(\hat{K}_\gamma \hat{K}_{\gamma'}^\dagger), \quad (5)$$

where the trace is taken in spin space.

WL and AL effects are obtained after energy average of $\mathcal{T}(E, \mathbf{B})$ for ballistic quantum dots (subject to an external arbitrarily directed magnetic field \mathbf{B}). The leading contributions after averaging (4) for a chaotic cavity with time-reversal symmetry, i.e., $\mathbf{B} = 0$, are as follows:

(i) The *classical* part consists of the terms $\gamma' = \gamma$ [9], for which the rapidly varying energy-dependent phase in the exponent of (4) disappears. Then the modulation factor is $\mathcal{M}_{\gamma,\gamma} = \text{Tr}(\hat{K}_\gamma \hat{K}_\gamma^\dagger) = 2s + 1$, independent of SO interaction, and reduces to the trivial spin degeneracy.

(ii) The *diagonal* quantum correction is defined for the reflection only. It contains the terms with $n = m$ and $\gamma' = \gamma^{-1}$, where γ^{-1} is the time-reversal of γ [9]. Again, the orbital phases of the trajectory pair cancel; however, the modulation factor is $\mathcal{M}_{\gamma,\gamma^{-1}} = \text{Tr}(\hat{K}_\gamma^2)$.

(iii) The *loop* contribution comes from pairs of long orbits that stay close to each other in configuration space, thereby have nearly equal actions, and hence persist upon energy average. One orbit of the pair has a self-crossing with a small crossing angle, thus forming a loop, while its partner exhibits an “anticrossing”. Outside the crossing region the orbits are located exponentially close to each other: the paths are related by time reversal along the loop and coincide along the rest of the trajectories [10, 16]. We have computed the modulation factor

for γ and γ' neglecting the crossing region and found $\mathcal{M}_{\gamma,\gamma'} = \text{Tr}(\hat{K}_l^2)$, where l is the loop segment of γ [14].

For spinless particles in chaotic quantum dots the three contributions to the averaged transmission and reflection yield [10], for $N = N' \gg 1$, (i) $\mathcal{T}_{\text{cl}}^{(0)} = \mathcal{R}_{\text{cl}}^{(0)} = N/2$, (ii) $\delta\mathcal{R}_{\text{diag}}^{(0)} = 1/2$, and (iii) $\delta\mathcal{T}_{\text{loop}}^{(0)} = \delta\mathcal{R}_{\text{loop}}^{(0)} = -1/4$, in agreement with RMT. Here the superscript refers to zero spin and zero magnetic field.

In the following, we consider the case of an additional uniform, arbitrarily directed magnetic field \mathbf{B} in the presence of SO interaction. Besides the Zeeman interaction, the field component B_z perpendicular to the cavity generates an additional Aharonov-Bohm (AB) phase factor $\varphi = \exp(i4\pi\mathbf{A}_\gamma B_z/\Phi_0)$ in the diagonal and loop terms in Eq. (4). Here, $\mathbf{A}_\gamma \equiv \int \mathbf{A} \cdot d\mathbf{l}/B_z$ is the effective enclosed area for the diagonal (loop) contributions accumulated along the orbits γ (loops l) neglecting bending of the orbits, and $\Phi_0 = hc/e$ is the flux quantum.

For broken time-reversal symmetry, e.g., by the perpendicular \mathbf{B} -field, $\mathcal{M}_{\gamma,\gamma'}$ should be calculated directly from (5). We then introduce a generalized modulation factor, $\mathcal{M}_\varphi \equiv \mathcal{M}_{\gamma,\gamma'}\varphi$, which is distributed according to a function $P(\mathcal{M}_\varphi; L, \mathbf{B})$, where L is the trajectory (loop) length in the diagonal (loop) contribution, and the \mathbf{B} -dependence includes both the AB phase and the Zeeman interaction. Thus we can define a spin modulation factor $\overline{\mathcal{M}_\varphi}(L; \mathbf{B})$ averaged over an ensemble of trajectories with fixed length L .

In chaotic systems, the length distribution is given by $\exp(-L/L_{\text{esc}})$ [9], if the escape length $L_{\text{esc}} = \pi\mathbf{A}_c/(w + w')$, the average length the particle traverses before leaving the cavity of area \mathbf{A}_c , is much larger than L_b , the average distance between two consecutive bounces at the boundaries. It can be shown [10, 14] that the relevant distribution of loop lengths is determined by the same exponent. As in the case without spin [9, 10], the product of the AB phase and spin modulation factors in Eq. (4) can be eventually substituted by its average $\langle \overline{\mathcal{M}_\varphi} \rangle_L$ over L and pulled out of the sum. Thereby we obtain, as relative quantum corrections for the spin- and \mathbf{B} -field-dependent transmission and reflection,

$$\begin{aligned} \delta\mathcal{R}_{\text{diag}}/\delta\mathcal{R}_{\text{diag}}^{(0)} &= \delta\mathcal{R}_{\text{loop}}/\delta\mathcal{R}_{\text{loop}}^{(0)} = \delta\mathcal{T}_{\text{loop}}/\delta\mathcal{T}_{\text{loop}}^{(0)} \\ &= \langle \overline{\mathcal{M}_\varphi}(\mathbf{B}) \rangle_L \equiv \frac{1}{L_{\text{esc}}} \int_0^\infty dL e^{-L/L_{\text{esc}}} \overline{\mathcal{M}_\varphi}(L; \mathbf{B}). \quad (6) \end{aligned}$$

Note that current conservation, i.e., $\delta\mathcal{R}_{\text{diag}} + \delta\mathcal{R}_{\text{loop}} = -\delta\mathcal{T}_{\text{loop}}$, is fulfilled in the semiclassical limit $N, N' \gg 1$. In the absence of SO interaction, we have $\overline{\mathcal{M}_\varphi}(L; \mathbf{B}) = (2s + 1) \exp(-\tilde{B}^2 L/L_b)$, where $\tilde{B} = 2\sqrt{2}\pi B_z \mathbf{A}_0/\Phi_0$ and \mathbf{A}_0 is the typical effective area enclosed, and the usual Lorentzian \tilde{B} -profile [9, 10] is recovered by Eq. (6).

In the case of SO interaction, the quantum corrections (6) depend on the modulation factor $\overline{\mathcal{M}_\varphi}(L; \mathbf{B})$, which characterizes the average spin evolution of a trajectory ensemble and can be easily determined from *clas-*

sical numerical simulations. Without \mathbf{B} -field, $\overline{\mathcal{M}}(L) \equiv \overline{\mathcal{M}_\varphi}(L; 0)$ changes from $\overline{\mathcal{M}}(0) = 2s + 1$ to the asymptotic value $\overline{\mathcal{M}}(\infty) = (-1)^{2s}$ [14]; i.e., for $s = 1/2$ an initial polarization ($\mathcal{M}(0) = 2$) becomes completely randomized ($\mathcal{M}(\infty) = -1$) owing to SO interaction, if the particle motion is irregular (see below). Thus, if the particle quickly leaves the cavity (large openings, small L_{esc}) or the SO interaction is too weak, there is not enough time for the modulation factor to deviate from $2s + 1$, giving rise to standard WL. In the opposite limit (large L_{esc} or relatively strong SO coupling) $\overline{\mathcal{M}}(L)$ quickly reaches its asymptotic value and, in view of (6), $\langle \overline{\mathcal{M}_\varphi}(0) \rangle_L \simeq (-1)^{2s}$. Hence for half-integer spin the conductance correction becomes positive due to SO interaction. This phenomenon of weak antilocalization does not exist for integer spin. For $\mathbf{B} \neq 0$ we find $\overline{\mathcal{M}_\varphi}(\infty; \mathbf{B}) = 0$ [14]: Both a magnetic flux (destroying constructive interference of the orbital phases) and the Zeeman interaction (affecting the spin phases) inhibit AL.

For a quantitative treatment we must specify the form of the SO interaction. In the following numerical analysis we consider the spin $s = 1/2$ -case for different quantum dot geometries and Rashba SO coupling [17], relevant for 2D semiconductor heterostructures. It is described by an effective magnetic field $\mathbf{C} = (2\alpha_R m_e / \hbar^2) \mathbf{v} \times \hat{\mathbf{z}}$, where α_R is the Rashba constant, m_e is the effective mass, and \mathbf{v} the (Fermi) velocity. In a billiard with fixed kinetic energy, \mathbf{C} is constant by magnitude and its direction changes only at the boundary. It is convenient to characterize the SO interaction strength by the mean spin-precession angle per bounce, $\theta_R = 2\pi L_b / L_R$, where $L_R = 2\pi |\mathbf{v}| / C$ is the Rashba length.

In the inset of Fig. 1 we plot the modulation factor $\overline{\mathcal{M}}(L)$ for three SO strengths for a chaotic, desymmetrized Sinai (DS) billiard (Fig. 1, geometry 2), i.e., a prototype of a geometry with hyperbolic classical dynamics. The average was performed over an ensemble of 10^5 (non-closed) trajectories (in the closed system) with random initial velocity directions and positions at the boundary. As θ_R increases, $\overline{\mathcal{M}}(L)$ reaches its asymptotic value -1 faster. In the main panel of Fig. 1 we compare, for fixed $\theta_R / 2\pi = 0.2$, $\overline{\mathcal{M}}(L)$ for four systems representing three different types of orbital motion:

Chaotic systems: Two representative geometries, the DS billiard (curve 2) and the desymmetrized diamond (DD) billiard [18] (curve 3), show up to deviations at small lengths nearly the same decay behavior of $\overline{\mathcal{M}}(L)$, indicating *universality* features for chaotic dynamics.

Integrable systems: Although Eq. (6) is valid only for chaotic cavities, the average modulation factor $\overline{\mathcal{M}}(L)$ is well defined for other types of motion. Remarkably, we find that for the integrable quarter-circle (QC) billiard (curve 1) $\overline{\mathcal{M}}(L)$ oscillates (with frequency independent of θ_R) around a constant saturation value well above -1 . A systematic analysis shows [14] that the saturation value in the integrable case is system-dependent and decreases

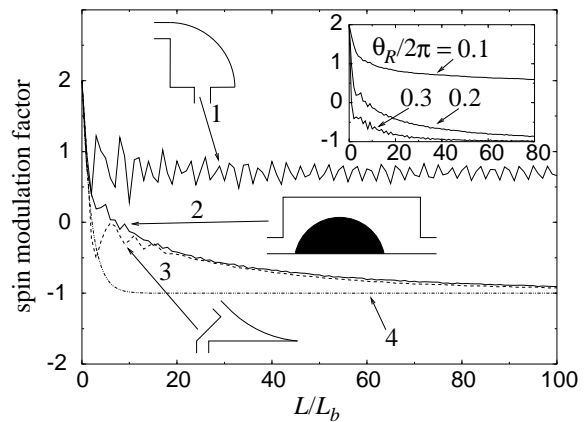


FIG. 1: Average modulation factor $\overline{\mathcal{M}}(L)$ as a function of orbit length L in units of bounce length L_b for the quarter-circle billiard (curve 1), the desymmetrized Sinai billiard (curve 2), the desymmetrized diamond billiard (curve 3), and for an unbounded diffusive system with mean-free path equal to L_b (analytical curve 4). The relative strength of spin-orbit interaction is $\theta_R / 2\pi = 0.2$. Inset: $\overline{\mathcal{M}}(L)$ for the desymmetrized Sinai billiard at different values of θ_R .

down to -1 , indicating spin relaxation, with increasing θ_R .

Diffusive systems: Unbounded diffusive motion (curve 4) exhibits fast exponential relaxation; i.e., $\overline{\mathcal{M}}(L) \simeq 3 \exp[-(\theta_R^2/3)(L/L_b)] - 1$ [14], where L_b is identified with the scattering mean-free path (cf. Eq. (10.12) of Ref. [2]).

Note that the curves 1-4 almost coincide for $L \lesssim L_b$, because up to the first scattering event the particle moves along a straight line, and different types of dynamics cannot be distinguished. On larger length scales, we find *significant qualitative and quantitative differences in the spin evolution in chaotic, integrable, and diffusive systems*. In particular, the relaxation is strongly suppressed for a confined, even chaotic, motion as compared to an unbounded diffusive motion with the same θ_R . This result is supported by the following argument: In the limit $\theta_R \ll 1$ the spin movements on the Bloch sphere “mimic” the orbital motion to order θ_R^2 ; i.e., they are bounded for a spatially confined system. If higher-order corrections were neglected, the spin relaxation would saturate at $L \sim L_b$. The further decrease of $\overline{\mathcal{M}}(L)$, of order $(L/L_b)\theta_R^4$, is due to a Berry phase acquired by the spin wave function [7, 8]. Its effect is similar to that of the AB phase. Hence, in a chaotic system without Zeeman interaction one finds [14]

$$\overline{\mathcal{M}_\varphi}(L; \mathbf{B}) \simeq e^{-(\tilde{B} + \tilde{\theta}_R^2)^2 L / L_b} + e^{-(\tilde{B} - \tilde{\theta}_R^2)^2 L / L_b}, \quad (7)$$

with $\tilde{\theta}_R^2 = (\mathbf{A}_0 / L_b^2) \theta_R^2 / \sqrt{2}$. The further relaxation is due to terms of order $(L/L_b)\theta_R^6$ [7, 8]. It eventually renders $\overline{\mathcal{M}}(L)$ negative and causes AL. For stronger interaction, $\theta_R \sim 1$, the three mechanisms (initial relaxation, Berry phase, and further relaxation) work simultaneously and cannot be separated (e.g., curves 2 and 3 in Fig. 1).

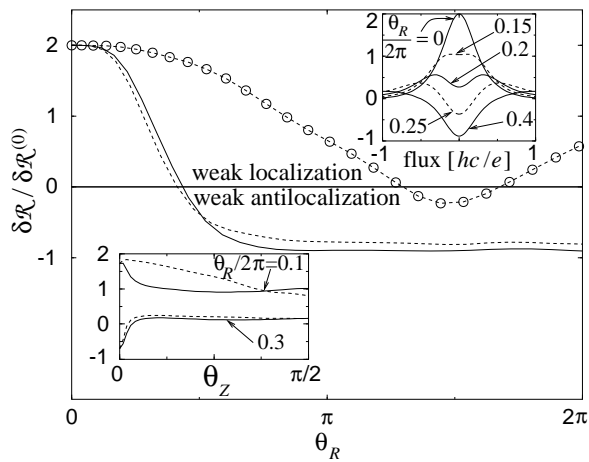


FIG. 2: Relative quantum correction to the reflection $\delta\mathcal{R}/\delta\mathcal{R}^{(0)}$ vs. spin-orbit interaction θ_R for $\mathbf{B} = 0$ in the desymmetrized Sinai (solid), diamond (dashed), and quarter-circle (dashed with circles) billiards with $P_c/(w+w') = 90$. Lower left inset: $\delta\mathcal{R}/\delta\mathcal{R}^{(0)}$ vs. Zeeman interaction θ_Z for the desymmetrized Sinai billiard. The in-plane field is directed parallel (solid) and perpendicular (dashed) to the long side. Upper right inset: $\delta\mathcal{R}/\delta\mathcal{R}^{(0)}$ vs. perpendicular magnetic flux for the same billiard with $\theta_Z = 0$.

Our numerical simulations show that in integrable systems both the spin direction and the phase oscillate almost periodically during the orbital motion. Therefore, after a short transient period, $\overline{\mathcal{M}}(L)$ usually saturates. One exception we found is the circular billiard. Here, owing to angular momentum conservation, all trajectories efficiently accumulate area, and $\overline{\mathcal{M}}(L) \simeq 2 \sin(x)/x$ for $\theta_R \ll 1$, where $x = \theta_R^2 L r / 2L_b^2$ and r is the radius [14].

Figure 2 shows the relative quantum correction to reflection, $\delta\mathcal{R}/\delta\mathcal{R}^{(0)}$, as a function of θ_R for chaotic and integrable geometries (at $\mathbf{B} = 0$). Positive (negative) values of $\delta\mathcal{R}/\delta\mathcal{R}^{(0)}$ indicate WL (AL). For chaotic systems $\delta\mathcal{R}/\delta\mathcal{R}^{(0)} \equiv (\delta\mathcal{R}_{\text{diag}} + \delta\mathcal{R}_{\text{loop}}) / (\delta\mathcal{R}_{\text{diag}}^{(0)} + \delta\mathcal{R}_{\text{loop}}^{(0)}) = \overline{\langle \mathcal{M}_\varphi \rangle}_L$ is given by Eq. (6). For the numerical calculation of $\overline{\mathcal{M}}(L)$ only (backscattered) orbits starting and ending at one lead are considered (since they are closed, the initial spin relaxation is reduced compared to non-closed paths). The chaotic DS (solid curve) and DD (dashed curve) billiards show a very similar WL-AL transition with increasing Rashba strength. The escape length in units of L_b is $P_c/(w+w')$, where P_c is the perimeter of the cavity. Hence, given L_R , one can also conclude that AL is absent in smaller quantum dots [for fixed $P_c/(w+w')$ or $w+w'$], as supported by experiment [5].

The results for the integrable QC billiard (dashed curve with circles) are based on a numerically obtained length distribution, which is no longer exponential. The transition to AL in the integrable billiard is much less pronounced and occurs at clearly higher θ_R , compared to its chaotic counterparts owing to the slower spin relaxation. Hence there exists an extended regime of SO strengths,

where one can switch from WL to AL by tuning the classical dynamics from integrable to chaotic.

The Zeeman interaction, measured by a precession angle θ_Z per bounce (analogous to θ_R), suppresses AL (lower left inset). Note the anisotropy in the (in-plane) field direction. The upper right inset depicts the magnetic-flux dependence. The characteristic double-peak structure follows from Eqs. (6) and (7).

The present semiclassical approach has a wider range of applicability, including ballistic integrable systems and SO strengths up to $\theta_R \sim 1$, compared to RMT [7, 8], which assumes $\theta_R \ll 1$ in the ballistic regime (Eq. (23) of [8]). Moreover, the RMT results contain free geometric parameters that have to be computed separately.

A corresponding analysis of ballistic conductance fluctuations [9] with spin appears promising. We expect the *shape* of its power spectrum to be independent of θ_R in an integrable system, but not in a chaotic system.

We thank M. Brack, A. V. Khaetskii, and M. Pletyukhov for stimulating discussions and P. Brouwer for a helpful clarification. The work has been supported by the Deutsche Forschungsgemeinschaft (OZ and KR) and the EU Spintronics Research Training Network (DF).

* E-mail: oleg.zaitsev@physik.uni-regensburg.de

- [1] G. Bergmann, Phys. Rep. **107**, 1 (1984).
- [2] S. Chakravarty and A. Schmid, Phys. Rep. **140**, 193 (1986).
- [3] Ch. Schierholz *et al.*, phys. stat. sol. (b) **233**, 436 (2002); J. B. Miller *et al.*, Phys. Rev. Lett. **90**, 076807 (2003); F. E. Meijer *et al.*, e-print cond-mat/0406106 (2004).
- [4] B. Hackens *et al.*, Phys. Rev. B **67**, 121403(R) (2003).
- [5] D. M. Zumbühl *et al.*, Phys. Rev. Lett. **89**, 276803 (2002).
- [6] A. V. Khaetskii and Y. V. Nazarov, Phys. Rev. B **61**, 12639 (2000); P. W. Brouwer, J. N. H. J. Cremers, and B. I. Halperin, Phys. Rev. B **65**, 081302 (2002); V. I. Fal'ko and T. Jungwirth, Phys. Rev. B **65**, 081306 (2002).
- [7] I. L. Aleiner and V. I. Fal'ko, Phys. Rev. Lett. **87**, 256801 (2001).
- [8] J.-H. Cremers, P. W. Brouwer, and V. I. Fal'ko, Phys. Rev. B **68**, 125329 (2003).
- [9] H. U. Baranger, R. A. Jalabert, and A. D. Stone, Phys. Rev. Lett. **70**, 3876 (1993); Chaos **3**, 665 (1993).
- [10] K. Richter and M. Sieber, Phys. Rev. Lett. **89**, 206801 (2002).
- [11] J. Bolte and S. Keppeler, Phys. Rev. Lett. **81**, 1987 (1998); Ann. Phys. (N.Y.) **274**, 125 (1999).
- [12] M. Pletyukhov and O. Zaitsev, J. Phys. A: Math. Gen. **36**, 5181 (2003); O. Zaitsev, *ibid* **35**, L721 (2002).
- [13] D. S. Fisher and P. A. Lee, Phys. Rev. B **23**, 6851 (1981).
- [14] O. Zaitsev, D. Frustaglia, and K. Richter (unpublished).
- [15] A similar Ansatz was used by C.-H. Chang, A. G. Mal'shukov, and K.-A. Chao, Phys. Lett. A, **326**, 436 (2004).
- [16] M. Sieber and K. Richter, Phys. Scr. **T90**, 128 (2001).
- [17] Y. Bychkov and E. Rashba, J. Phys. C **17**, 6039 (1984).
- [18] S. Müller, Eur. Phys. J. B **34**, 305 (2003).